

ASP: Learn a Universal Neural Solver!

Chenguang Wang, Zhouliang Yu, Stephen McAleer,
Tianshu Yu, and Yaodong Yang

Abstract—Applying machine learning to combinatorial optimization problems has the potential to improve both efficiency and accuracy. However, existing learning-based solvers often struggle with generalization when faced with changes in problem distributions and scales. In this paper, we propose a new approach called ASP: **Adaptive Staircase Policy Space Response Oracle** to address these generalization issues and learn a universal neural solver. ASP consists of two components: Distributional Exploration, which enhances the solver’s ability to handle unknown distributions using Policy Space Response Oracles, and Persistent Scale Adaption, which improves scalability through curriculum learning. We have tested ASP on several challenging COPs, including the traveling salesman problem, the vehicle routing problem, and the prize collecting TSP, as well as the real-world instances from TSPLib and CVRPLib. Our results show that even with the same model size and weak training signal, ASP can help neural solvers explore and adapt to unseen distributions and varying scales, achieving superior performance. In particular, compared with the same neural solvers under a standard training pipeline, ASP produces a remarkable decrease in terms of the optimality gap with 90.9% and 47.43% on generated instances and real-world instances for TSP, and a decrease of 19% and 45.57% for CVRP.

Index Terms—Combinatorial Optimization Problems, Curriculum Learning, Policy Space Response Oracles, Generalization Ability and Scalability



1 INTRODUCTION

COMBINATORIAL optimization problems (COPs) have received significant attention from the operation research (OR) and theoretical computer science (TCS) communities due to their numerous applications. Both OR and TCS have developed a variety of solvers to tackle COPs, including both exact and heuristic approaches. However, the design of these solvers is extremely labor-intensive and requires extensive domain knowledge, making it difficult to create new solvers.

Recently, COPs have also attracted attention from the machine learning community, as it was discovered that deep learning-based “neural solvers” can capture complex structures and heuristics through the analysis of large numbers of problem instances [1]. These neural solvers have been found to be very efficient on large-scale problems, and have the added benefit of relieving the tedious labor required to design traditional solvers. However, current neural solvers suffer from generalization issues in two main areas: problem distribution and scalability.

Almost all previous neural solvers have been trained and tested on a well-defined problem distribution and scale, and do not perform well when applied to real-world scenarios where the problem distribution and scale can vary significantly [1], [2], [3], [4], [5]. This limits the use of neural solvers as alternatives or replacements for traditional solvers. One potential solution to the generalization issues faced by previous neural solvers is to train different solvers for different settings or to use a very large model that

can handle a wide range of problem instances. However, these approaches have drawbacks. Training multiple solvers can be computationally intensive and require significant resources, while using a very large model can sacrifice efficiency and may result in degraded performance when adapting to different settings. As a result, we are interested in the following question:

- *Can we obtain a capacity-efficient neural solver without sacrificing performance while overcoming distributional and scale issues?*

Several recent studies have attempted to address the generalization issues faced by previous neural solvers for COPs, but from specific angles. For example, some research has focused on creating new distributions during training to address the issue of data distribution [6], [7], while others have examined ways to adapt neural solvers to different scales [8]. However, none of these methods offer a comprehensive, systematic approach to addressing the generalization issues universally.

In this paper, we propose a new method called ASP: Adaptive Staircase Policy Space Response Oracle (PSRO), which aims to address the generalization issues faced by previous neural solvers and provide a “universal neural solver” that can be applied to a wide range of problem distributions and scales. Our method incorporates game theory and curriculum learning, and demonstrates improved performance on a variety of COPs compared to traditional solvers and previous neural solvers. Specifically, our method follows the two-player zero-sum meta-game framework proposed in [6], and employs policy space response oracles (PSROs) to adapt to different problem distributions and scales. We also introduce the concept of a staircase policy [9], which allows our method to learn multiple policies at once and make more efficient use of the model’s capacity.

- Chenguang Wang, Zhouliang Yu and Tianshu Yu are with School of Data Science, the Chinese University of Hongkong, Shenzhen, China. E-mail: {chenguangwang, zhouliangyu}@link.cuhk.edu.cn, yu-tianshu@cuhk.edu.cn
- Stephen McAleer is with Carnegie Mellon University, USA. E-mail: smcaleer@cs.cmu.edu
- Yaodong Yang is with Institute for AI, Peking University, Beijing, China. E-mail: yaodong.yang@pku.edu.cn

ASP consists of two main components: Distributional Exploration (DE) and Persistent Scale Adaption (PSA). DE uses policy space response oracles (PSROs) to adapt the neural solver to different problem distributions, while PSA uses an adaptive staircase procedure to gradually increase the difficulty of the problem scale, allowing the neural solver to persistently improve its performance on a wide range of scales. Different from [6] which generates the attack distribution by learning mixed Gaussian perturbations and approximating policy gradient via the Monte Carlo method, we utilize Real-NVP [10], a more generic generation approach via Normalizing Flow which can generate various data distributions with exact probability.

We have tested ASP on several classical COPs, including the traveling salesman problem (TSP) and the capacitated vehicle routing problem (CVRP), using two typical RL-based neural solvers: Attention Model (AM) [2] and POMO [5]. Our results show that ASP can achieve impressive improvements compared to the original solvers trained under standard paradigms, and outperforms all other DL-based neural solvers on both TSPLib [11] and CVRPLib [12] datasets. Additionally, we have conducted ablation studies to demonstrate the effectiveness of our approach and the influence of model capacity on training.

In summary, our main contributions are as follows:

- We propose the ASP framework, which is designed to overcome the generalization issues faced by previous neural solvers for COPs. This framework is model- and problem-agnostic, making it widely applicable to a range of neural solvers and COPs.
- Without increasing the model capacity, ASP allows a neural solver to discover complex structures by interchangeably learning from different distributions and scales, resulting in state-of-the-art performance even with comparable training resources to other methods trained under a fixed setting.
- We conduct extensive ablation studies and provide insights into training strategy design, model capacity, the function landscape of COPs, and beyond. These findings can broaden the horizons of future research in the field of COPs.

2 RELATED WORK

Deep Learning for Combinatorial Optimization Problems

- Pointer Networks [13] is the first attempt to solve COPs with deep learning, specifically by training a pair of RNN-based encoder and decoder to output a permutation over its inputs. [14] applies a similar model but instead trained the model with reinforcement learning rather than supervised learning used in Pointer Networks, by treating the tour length following the node sequence as the reward signal. Inspired by the success of Transformers [15], Attention Model [2] uses the attention mechanism, which is similar to Graph Attention Networks [16], to encode the node representation and decode the solutions to various problems. [17] proposes the “Learn to Improve” (L2I) model which iteratively refines the solution with improvement operators, and jumps out of local optima with perturbation operators. Similarly, [3] proposed a reinforcement learning framework

to learn the improvement heuristics for TSP and the Capacitated Vehicle Routing Problem (CVRP) and achieves excellent results both on randomly generated instances and real-world instances. Some recent works [4], [18], [19], [20] focus on pretraining models and constructing heatmaps to guide the search method. Although deep learning- or reinforcement learning-based methods have achieved notable progress in various COPs, in addition to generalization issues, some other essential limitations also exist, for example, degenerated performance on large-scale problems and high computational consumption during training. Finally, we refer to [21] for a comprehensive review of the existing challenges in this area.

Generating Hard Instances - There are some previous works that seek to obtain robust algorithms by generating hard-to-solve instances [22], [23], [24]. [22] proposed a method to generate a representation of the problem instance space, with which the performance of certain algorithms can be quantified and thus the generalization can be inferred. Using the measurable features, they can analyze the similarities and differences between instances and the strengths and weaknesses of algorithms. Closely related to our work, [23] focuses on AdWords problem and constructs an adversarial training framework inspired by game theory, which employs GANs [25] to generate adversarial instances to expose the weakness of any given algorithms. [24] considers the instance generation and portfolio construction in an adversarial fashion to reduce the impact of deviation of training data. Different from these works, we adopt the PSRO [26] framework to obtain a population of learnable solvers through meta-game and devise a model mixture method to combine these solvers, which leads to state-of-the-art performance. In future work we will investigate applying new PSRO variants for improved performance [27], [28], [29]. One could also potentially apply other algorithms for two-player zero sum games to our objective [30], [31], [32].

Curriculum Learning - [33] firstly propose the concept of curriculum learning (CL) where a machine learning algorithm should be trained from easy tasks to hard tasks. Being a plug-and-play module with high flexibility, curriculum learning has been broadly used in various research fields: computer vision [34], [35], natural language processing [36], [37], reinforcement learning (RL) [38], [39], [40], [41], [42], to name a few. Numerous successful applications of CL have demonstrated its capability of improving the performance on target tasks and accelerating the convergence of training process. Specifically for RL, CL can improve sample efficiency and asymptotic performance which are considered beneficial for the exploration and generalization [41]. Closely related to our work, [7] introduces “adaptive-hardness” to assess the generalizability of the neural solver and proposes a curriculum learner to improve the neural solver’s generalizability over data distribution. [8] instead utilizes curriculum learning to improve the scalability of neural solvers. But these two works are limited to only one dimension of generalization issues respectively: [7] focuses on generating hard instances with respect to the data distribution; [8] cares more about the problem scale. In this work, we take these two dimensions into consideration together.

3 NOTATIONS AND PRELIMINARIES

Normal Form Game (NFG) - A tuple (Π, \mathbf{U}^Π, n) where n is the number of players, $\Pi = (\Pi_1, \Pi_2, \dots, \Pi_n)$ is the joint policy set and $\mathbf{U}^\Pi = (\mathbf{U}_1^\Pi, \mathbf{U}_2^\Pi, \dots, \mathbf{U}_n^\Pi) : \Pi \rightarrow \mathbb{R}^n$ is the utility matrix for each joint policy. A game is symmetric if all players have the same policy set ($\Pi_i = \Pi_j, i \neq j$) and same payoff structures, such that players are interchangeable.

Best Response - The strategy which attains the best expected performance against a fixed opponent strategy. $\sigma_i^* = \text{br}(\Pi_{-i}, \sigma_{-i})$ is the best response to σ_{-i} if:

$$\mathbf{U}_i^\Pi(\sigma_i^*, \sigma_{-i}) \geq \mathbf{U}_i^\Pi(\sigma_i, \sigma_{-i}), \forall i, \sigma_i \neq \sigma_i^*$$

Nash Equilibrium - A strategy profile $\sigma^* = (\sigma_1^*, \sigma_2^*, \dots, \sigma_n^*)$ such that:

$$\mathbf{U}_i^\Pi(\sigma_i^*, \sigma_{-i}^*) \geq \mathbf{U}_i^\Pi(\sigma_i, \sigma_{-i}^*), \forall i, \sigma_i \neq \sigma_i^*$$

Intuitively, no player has an incentive to deviate from their current strategy if all players are playing their respective Nash equilibrium strategy.

Traveling Salesman Problem (TSP) - The objective is to find the shortest route that visits each location only once and return to the original location. In this paper, we only consider the two-dimension euclidean case, that is, each location's information comprises $(x_i, y_i) \in \mathbb{R}^2$.

Vehicle Routing Problem (VRP) - In the Capacitated VRP (CVRP) [43], there is a depot node and several demand nodes, the vehicle starts and ends at the depot node in multiple routes where the total demand of the demand nodes in each route does not exceed the vehicle capacity. The objective of the CVRP is to minimize the total route cost while satisfying all the constraints. We also consider the Split Delivery VRP (SDVRP), which allows to split customer demands over multiple routes.

Prize Collecting TSP (PCTSP) - In the PCTSP [44], the salesman who travels the given two-dimension locations, gets a prize in each location that he visits and pays a penalty to those that he fails to visit. The objective is to minimize the traveling length and penalties, while visiting enough cities to collect a prescribed amount of prizes. We also consider the Stochastic PCTSP (SPCTSP) in which the expected location prize is known upfront, but the real collected prize only becomes known upon visitation.

Instance - An individual sample of a combinatorial optimization problem. For example, given the two-dimensional coordinates of n points, finding the shortest tour that traverses all points is an instance of TSP. Hereafter, we denote an instance with problem scale n by \mathcal{I}^n which comes from some distribution $\mathbf{P}_{\mathcal{I}^n}$.

Optimality gap - Measures the quality of a solver compared to an optimal oracle. Given an instance \mathcal{I}^n and a solver $S : \{\mathcal{I}^n\} \rightarrow \mathbb{R}$, the optimality gap is defined as:

$$g(S, \mathcal{I}^n, \text{Oracle}) = \frac{S(\mathcal{I}^n) - \text{Oracle}(\mathcal{I}^n)}{\text{Oracle}(\mathcal{I}^n)} \quad (1)$$

where $\text{Oracle}(\mathcal{I}^n)$ gives the true optimal value of the instance. Furthermore, the *expected* optimality gap of solver under an instance distribution $\mathbf{P}_{\mathcal{I}^n}$ is defined as:

$$G(S, \mathbf{P}_{\mathcal{I}^n}, \text{Oracle}) = \mathbf{E}_{\mathcal{I}^n \sim \mathbf{P}_{\mathcal{I}^n}} g(S, \mathcal{I}^n, \text{Oracle}). \quad (2)$$

Algorithm 1 Distributional Exploration (DE) with PSRO

Input: Neural Solver S , problem scale n
Initialize: Joint policy set $\Pi = \{(S^n, \mathbf{P}_{\mathcal{I}^n})\}$, utility matrix \mathbf{U}^Π , meta-strategies $\sigma = (\sigma_{\text{SS}}, \sigma_{\text{DG}})$
while epoch e in $\{1, 2, \dots\}$ **do**
 Train Oracles: $(S', \mathbf{P}'_{\mathcal{I}^n})$ under problem scale n w.r.t. Eq. 5 and Eq. 8
 Update policy set: $\Pi \leftarrow \Pi \cup \{(S', \mathbf{P}'_{\mathcal{I}^n})\}$
 Update \mathbf{U}^Π from new Π and compute the new meta-strategy σ
end while
Output: The best solver S_{best}^n chosen from Π_{SS} and mixed distribution $\mathbf{P}^n = \sum_i \sigma_{\text{DG}, i} \mathbf{P}_{\mathcal{I}^n, i}$

4 METHOD

In this section, we present the framework, ASP, to obtain a universal neural solver with strong generalization ability on distribution and scale. In general, ASP contains two major components: **(1)** Distributional Exploration (DE): PSRO-based training for the improvement over distribution changes under a specific problem scale; and **(2)** Persistent Scale Adaption (PSA): Adaptive Staircase based curriculum for enhancing the generalization on a range of problem scales. The overview of ASP is shown in Fig. 1. In the following parts, we will elaborate on them in detail.

4.1 Distributional Exploration

In this section, we formulate Distributional Exploration as a two-player game at the meta-level to improve the neural solver's generalization ability on the distribution dimension. When handling COP instances with problem scale n , we assume there are two players in the meta-game:

- $\Pi_{\text{SS}} = \{S_i^n \mid i = 1, 2, \dots\}$ is the policy set for the Solver Selector where S_i^n is the neural solver;
- $\Pi_{\text{DG}} = \{\mathbf{P}_{\mathcal{I}^n, i}, i = 1, 2, \dots\}$ is the instance distribution policy set where $\mathbf{P}_{\mathcal{I}^n, i}$ is the instance distribution under problem scale n .

Formally, we have a two player asymmetric NFG $(\Pi, \mathbf{U}^\Pi, 2)$, $\Pi = (\Pi_{\text{SS}}, \Pi_{\text{DG}})$ is the joint policy set and $\mathbf{U}^\Pi : \Pi \rightarrow \mathbb{R}^{|\Pi_{\text{SS}}| \times |\Pi_{\text{DG}}|}$ is the utility matrix. Given a joint policy $\pi = (S^n, \mathbf{P}_{\mathcal{I}^n}) \in \Pi$, its utility is given by

$$\mathbf{U}^\Pi(\pi) = (\mathbf{U}^{\Pi_{\text{SS}}}(\pi), \mathbf{U}^{\Pi_{\text{DG}}}(\pi))$$

where $\mathbf{U}^{\Pi_{\text{SS}}}(\pi) = -\mathbf{U}^{\Pi_{\text{DG}}}(\pi) = -G(\pi, \text{Oracle})$ is the expected optimality gap under the joint policy π as defined in Eq. 2. The overall objective in the meta-level is:

$$\min_{\sigma_{\text{SS}} \in \Delta(\Pi_{\text{SS}})} \max_{\sigma_{\text{DG}} \in \Delta(\Pi_{\text{DG}})} \mathbf{E}_{\pi \sim (\sigma_{\text{SS}}, \sigma_{\text{DG}})} G(\pi, \text{Oracle}). \quad (3)$$

where $\Delta(\cdot)$ denotes the distribution on the given set. We obey the PSRO framework as follows: at each iteration given the policy sets $\Pi = (\Pi_{\text{SS}}, \Pi_{\text{DG}})$ and the meta-strategy $\sigma = (\sigma_{\text{SS}}, \sigma_{\text{DG}})$, we train two Oracles:

- S' represents a new neural solver, which is the best response to the meta-strategy σ_{DG} .
- $\mathbf{P}'_{\mathcal{I}^n}$ represents a new instance distribution where Solver Selector performs poorly when following σ_{SS} .

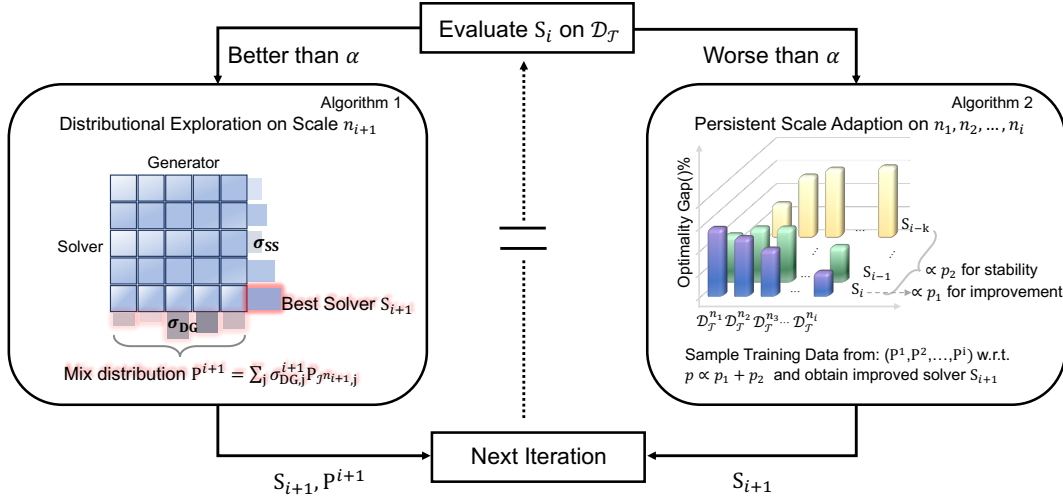


Fig. 1: The pipeline of ASP framework. At the i -th iteration, ASP chooses to either improve the generalization ability on a larger problem scale n_{i+1} or enhance the generalization ability on a set of pre-selected problem scales, depending on whether the performance of the current neural solver on the evaluation set is better than the preset threshold α . If the performance is better than α , we conduct the DE procedure on scale n_{i+1} , as detailed in algorithm 1, obtaining the best solver S_{i+1} and mixed data distribution P^{i+1} according to the meta-strategy. If not, we turn to improve S_i 's ability with the PSA procedure by training on problem scales n_1, n_2, \dots, n_i , as detailed in algorithm 2. To sample training data from P^j under problem scale n_j , we propose a sample strategy (Eq. 12) based on the current and historical performance on evaluation set which balances the tendency of improvement and stability. Then an enhanced solver S_{i+1} is obtained for the next iteration.

Given these oracles, we update the joint policy set $\Pi \leftarrow \Pi \cup (S', \mathbf{P}'_{\mathcal{I}^n})$ and the meta-game \mathbf{U}^Π according to new Π . This expansion of the joint policy set has a dual purpose in that it aids in finding the difficult-to-solve instance distributions whilst also improving the ability of the Solver Selector to handle them. The general algorithm framework can be seen in Alg. 1.

The formulation above leaves us with three algorithmic components to address: **(1)** How to obtain the meta-strategy σ ; **(2)** How to train Oracles for each player; **(3)** How to evaluate the utilities \mathbf{U}^Π . In the following parts, we will describe the flow of the algorithm.

Meta-Strategy Solvers - Given that we formulate a two-player game in Eq. 3, it's preferable to use Nash Equilibrium of the meta-game as the meta-strategy solution due to its computational efficiency.

Oracle Training - We now provide the higher-level results for training a best-response Oracle, with more detailed derivations presented in Appendix A. Here we represent the neural solvers in Π_{SS} as S_θ and the instance distributions in Π_{DG} as $\mathbf{P}_{\mathcal{I}^n, \gamma}$ where θ and γ are the trainable parameters.

- For solver Oracle: Given the meta-strategy σ_{DG} , the oracle training objective for the neural solver is:

$$\min_{\theta} L_{SS}(\theta) = \mathbf{E}_{\mathbf{P}_{\mathcal{I}^n} \sim \sigma_{DG}} G(S_\theta, \mathbf{P}_{\mathcal{I}^n}, \text{Oracle}). \quad (4)$$

We can optimize this objective by stochastic gradient descent and the gradient is:

$$\nabla_{\theta} L_{SS}(\theta) = \mathbf{E}_{\mathbf{P}_{\mathcal{I}^n} \sim \sigma_{DG}} \mathbf{E}_{\mathcal{I}^n \sim \mathbf{P}_{\mathcal{I}^n}} \frac{\nabla_{\theta} S_{\theta}(\mathcal{I}^n)}{\text{Oracle}(\mathcal{I}^n)}. \quad (5)$$

Given that it's impossible to call "Oracle" in Eq. 5 for excessively numerous iterations during training, we can alternatively train solver Oracle to obtain a powerful neural solver given distribution $\mathbf{P}_{\mathcal{I}^n}$ with the gradient:

$$\nabla_{\theta} L_{SS}(\theta) = \mathbf{E}_{\mathbf{P}_{\mathcal{I}^n} \sim \sigma_{DG}} \mathbf{E}_{\mathcal{I}^n \sim \mathbf{P}_{\mathcal{I}^n}} \nabla_{\theta} S_{\theta}(x_1, \dots, x_n). \quad (6)$$

- For data generator Oracle: Given the meta-strategy σ_{SS} , the oracle training objective for the DG is:

$$\max_{\gamma} L_{DG}(\gamma) = \mathbf{E}_{S \sim \sigma_{SS}} G(S, \mathbf{P}_{\mathcal{I}^n, \gamma}, \text{Oracle}). \quad (7)$$

The gradient w.r.t. γ is:

$$\nabla_{\gamma} L_{DG}(\gamma) = \mathbf{E}_{S \sim \sigma_{SS}} \mathbf{E}_{\mathcal{I}^n \sim \mathbf{P}_{\mathcal{I}^n, \gamma}} \left[\nabla_{\gamma} (\log \mathbf{P}_{\mathcal{I}^n, \gamma}(\mathcal{I}^n)) g(S, \mathcal{I}^n, \text{Oracle}) \right]. \quad (8)$$

Similar with the training oracles for the neural solver, we can omit the call of the Oracle solver as well. Otherwise, to accurately calculate the probability $\mathbf{P}_{\mathcal{I}^n, \gamma}(\mathcal{I}^n)$ in Eq. 8, we apply Real-NVP [10], a Normalizing Flow-based generative model to generate adversarial data. Concretely, we start from a simple prior probability distribution

$$z \sim p_Z = \text{Uni}([0, 1]^k) \quad (9)$$

with the probability $p_Z(z) = 1, \forall z \in [0, 1]^k$ where k is the dimension of input feature. We obtain the adversarial data by a parameterized bijection

$$x = G_{\gamma}(z) : Z \rightarrow X,$$

then the exact probability of obtaining x is given by the change of variable formula:

$$p_X(x) = p_Z(G^{-1}(x)) \left| \det \left(\frac{\partial G_\gamma^{-1}}{\partial x} \right) \right| = \left| \det \left(\frac{\partial G_\gamma^{-1}}{\partial x} \right) \right|.$$

This probability can be computed efficiently and exactly thanks to the construction of f_γ in Real-NVP, so we are able to calculate the probability $\mathbf{P}_{\mathcal{I}^n, \gamma}(\mathcal{I}^n)$ in this way.

Evaluation - Given the joint policy $\pi \in \Pi$, we can compute the element in the utility matrix $\mathbf{U}^\Pi(\pi) = (-G(S, \mathbf{P}_{\mathcal{I}^n}, \text{Oracle}), G(S, \mathbf{P}_{\mathcal{I}^n}, \text{Oracle}))$ by approximating the expected optimality gap defined in Eq. 2:

$$\begin{aligned} G(S, \mathbf{P}_{\mathcal{I}^n}, \text{Oracle}) &= \mathbf{E}_{\mathcal{I}^n \sim \mathbf{P}_{\mathcal{I}^n}} g(S, \mathcal{I}^n, \text{Oracle}) \\ &\approx \frac{1}{M} \sum_{i=1}^M g(S, \mathcal{I}_i^n, \text{Oracle}). \end{aligned} \quad (10)$$

where $S \in \Pi_{\text{SS}}, \mathbf{P}_{\mathcal{I}^n} \in \Pi_{\text{DG}}$.

After finishing the training of PSRO for problem scale n , we obtain the best neural solver S_{best}^n and a mixed distribution $\mathbf{P}^n = \sum_i \sigma_{\text{DG}, i} \mathbf{P}_{\mathcal{I}^n, i}$ for later usage.

4.2 Persistent Scale Adaption

Algorithm 2 Task Selection by Persistent Scale Adaption (PSA)

Input: Neural Solver S , a range of problem scales n_1, \dots, n_i and mixed distributions $\mathbf{P}^1, \dots, \mathbf{P}^i$

Initialize: $p_0 \in \mathbb{R}^i$ with a uniform probability vector

while epoch t in $\{1, 2, \dots\}$ **do**

 Evaluate S on each (\mathbf{P}^k, n_k) by Eq. 10 to obtain cost vector $c^t = (c_k^t)_k$

 Compute the task selection strategy p_t followed by Eq. 12 and train a new neural solver S^t w.r.t. Eq. 11 with

$P_{\text{PS}} = p_t$

 Assign $S \leftarrow S^t$

end while

Output: The new trained Neural Solver S .

Considering a range of problem scales (n_1, n_2, \dots, n_i) , we want to obtain a universal neural solver which has persistent performance on all problem scales. In this section, we propose the Persistent Scale Adaption (PSA) procedure to achieve this under the framework of curriculum learning. Concretely, we can formulate this as a multi-objective problem:

$$\min_{\theta} L_{\text{PSA}}^M(\theta) = (G(S_\theta, \mathbf{P}^{n_1}, \text{Oracle}), \dots, G(S_\theta, \mathbf{P}^{n_i}, \text{Oracle})).$$

A common way to optimize this is transferring it to a single objective problem by assigning each objective a weight, leading to the expectation form:

$$\min_{\theta} L_{\text{PSA}}(\theta) = \mathbf{E}_{n \sim P_{\text{PS}}} G(S_\theta, \mathbf{P}^n, \text{Oracle}). \quad (11)$$

where P_{PS} is the task selection strategy, a discrete probability distribution over the problem scales (n_1, n_2, \dots, n_i) such that $P_{\text{PS}}(n = n_k) = p_k, \sum_k p_k = 1$. There are many candidates for P_{PS} , e.g. the uniform distribution as in the original Adaptive Staircase Procedure, but this would mislead the

neural solver training on improper tasks. Here we propose a *momentum-based* mechanism to guide the neural solver to focus on the proper tasks.

We treat the sampling probability $\{p_i\}$ as a weak signal to guide training process towards the improvement on target distribution $\mathcal{D}_{\mathcal{T}}$. By evaluating the neural solver S_θ on each pair of $(\mathcal{D}_{\mathcal{T}}, n_k)$ we can obtain a cost vector $c \in \mathbb{R}^i$:

$$c = (c_k)_k, \text{ where } c_k \text{ is evaluated by Eq. 10,}$$

measuring the performance of S_θ on the data distribution $\mathcal{D}_{\mathcal{T}}$ under the problem scale n_k . During the implementation, we will execute the PSA procedure until reaching some conditions (e.g., achieving the pre-set performance or conducting the training for certain iterations), so we denote the cost vector at the t -th PSA iteration as $c^t = (c_k^t)_k$ and construct $\{p_i^t\}$ as follows:

$$p_i^t \propto \lambda p_i^1 + (1 - \lambda) p_i^2, \lambda \in [0, 1] \quad (12)$$

where $p_i^1 \propto \lfloor c_i^t - c_i^{t-1} \rfloor_+$ with $\lfloor x \rfloor_+ = x$ if $x > 0$, otherwise 0; $p_i^2 \propto \sqrt{\text{Var}_t[c_i^t]}$. p_i^1 helps us focus on the problem scales on which the neural solver performs poorly and p_i^2 measures the stability over history performance, which benefits the training process with more stability. λ is the weight to balance the two terms.

Since c^t is unknown beforehand and changes over training time, we maintain a history of the previous 10 steps of cost vectors, and update $\text{Var}_t[c_i^t]$ dynamically during training, so that we can guide the training process to focus on those tasks on which the performance is unsatisfactory and unstable. At the beginning of training, we sample n_i uniformly. The whole process can be seen in Alg. 2.

4.3 The Whole ASP Pipeline

In this section, we provide the overall details of the Adaptive Staircase PSRO (ASP) framework by integrating the components in previous sections.

Borrowing the idea from curriculum learning that starting from easy tasks and raising the difficulty level gradually, we begin to train the neural solver from the smallest problem scale because problems with larger scales are considered to be harder than smaller ones in the context of COPs. Inspired by Adaptive Staircase Procedure [9], at each ASP iteration, we consider two optional procedures: DE procedure described in algorithm 1 and PSA procedure described in algorithm 2. Given the problem scales we have handled (n_1, n_2, \dots, n_i) and neural solver S_θ trained so far, if the evaluation results of S_θ on target distribution $\mathcal{D}_{\mathcal{T}}$ is better than a preset threshold α , we will conduct DE procedure on a larger problem scale n_{i+1} , meaning taking a higher staircase to a harder task, otherwise we invoke PSA procedure on (n_1, n_2, \dots, n_i) , meaning enhancing S_θ 's ability on current tasks. We repeat this process until some stop criterion is satisfied and the whole pipeline is shown in Alg. 3.

5 EXPERIMENTS

In this section, we present our results on several COPs: TSP, CVRP, SDVRP, PCTSP, and SPCTSP. In contrast to previous work which fails to show generalization ability due to

Algorithm 3 ASP (Adaptive-Stairs PSRO)

Input: Neural Solver S , minimal and maximal problem scale n_1, n_K , incremental step n_{step} , evaluation dataset $D = \{\mathcal{D}_{\mathcal{T}}^{n_1}, \mathcal{D}_{\mathcal{T}}^{n_1+n_{\text{step}}}, \dots, \mathcal{D}_{\mathcal{T}}^{n_K}\}$ and performance threshold α , training patience γ

Initialize: Problem scale list $p_l = [n_1]$, $S_{\text{best}}, \mathbf{P}^1 = \text{DE}(S, n_1)$ by Alg. 1, mix distribution list $p_{\text{dist}} = [\mathbf{P}^1]$, count=0, evaluate S_{best} on $\mathcal{D}_{\mathcal{T}}^{n_1}$ to get evaluation result r

while True **do**

if ($r \leq \alpha$ or count $> \gamma$) and $p_l[-1] \leq n_K$ **then**

$n' = p_l[-1] + n_{\text{step}}$

if $n' < n_K$ **then**

$p_l \leftarrow p_l + [n']$

else

 Break

end if

$S_{\text{best}}, \mathbf{P}^{\text{new}} = \text{DE}(S_{\text{best}}, p_l[-1])$ by Alg. 1

$p_{\text{dist}} \leftarrow p_{\text{dist}} + [\mathbf{P}^{\text{new}}]$

 count+=1

else

$S_{\text{best}} = \text{PSA}(S_{\text{best}}, p_l, p_{\text{dist}})$ by Alg. 2

 count+=1

end if

 Evaluate S_{best} on $\{\mathcal{D}_{\mathcal{T}}^{n_1}, \dots, \mathcal{D}_{\mathcal{T}}^{p_l[-1]}\}$ to get evaluation result r

end while

Output: The best Neural Solver S_{best}

training and testing on the same distribution (uniform) and training a model for each problem scale, we demonstrate performance on distributions that are *never trained* and evaluate *only one* model on various problem scales.

5.1 Experimental Settings

Base Solver - Our method is model- and problem-agnostic so we employ existing neural solvers on various COPs to demonstrate the validity of this framework. We call the neural solver without the training of our method as *base solver* and denote the neural solver using our method with the annotation *base solver(ASP)*.

COP	Base Solver	Threshold
TSP	AM [2]	3
	POMO [5]	0.5
CVRP	AM [2]	5
	POMO [5]	1
SDVRP	AM [2]	10
PCTSP	AM [2]	10
SPCTSP	AM [2]	10

TABLE 1: Base solver and threshold for each COP

Training Setting - All the training under different base solvers and COPs is from scratch. Considering the different performance of neural solvers on different COPs, the choices of base solvers for each COP and settings of performance threshold α are different as well, as shown in Table 1. For the weight in Eq. 12, we use $\lambda = 0.5$ for all experiments. We set the minimal and maximal problem scale $n_1 = 20, n_K = 100$, and incremental step $n_{\text{step}} = 20$ for all COPs. During the

training process, we evaluate the neural solver on target distribution $\mathcal{D}_{\mathcal{T}}$ under the problem scales that have never been trained and get average evaluation result r . A patience parameter $\gamma = 5$ is also set to prevent the neural solver from getting stuck in the current tasks, that is, we will step to a harder task if no further improvements are observed after 5 training iterations of the PSA procedure.

The Data Generator is a Normalizing Flow-based model, Real-NVP [10] with 5 coupling layers and we train its parameters using Adam optimizer [45] with a learning rate of $1e-4$ for 100 epochs. What’s more, we reset the parameters when we begin to conduct DE training for a larger problem scale. We leave the detailed settings about model structure and training configurations for base solvers and data generator in Appendix B

Baselines - For TSP, we compare the solution quality and inference speed of the neural solvers trained by our framework with exact solvers, non-learning-based heuristics methods, and learning-based methods. More specifically, the counterpart solvers include Concorde, Gurobi [46], LKH3 [47] which is a state-of-the-art heuristic solver, and OR-tools which is an approximate solver based on meta-heuristics. Moreover, we also compare against Nearest, Random, and Farthest Insertion. Additionally, we compare our methods with a variety of learning-based methods: LIH [17], AM [2], MDAM [48], POMO [5], GCN [49] and CVAE-opt [50]. For CVRP, we test the performance of the neural solvers trained by ASP in comparison with the following solvers: LKH3, and Gurobi with various time limits, as well as the following mentioned learning-based methods: AM, POMO, RL(gr.) [51], NeuRewriter [52] and CVAE-opt. For SDVRP, we compare against RL(gr.), AM [2], and MDAM [48]. For PCTSP, we compare against Gurobi, OR-Tools, as well as the python version of Iterated Local Search(ILS). Moreover, we also compare our neural solver AM(ASP) to its baseline, AM [2]. For SPCTSP, We compare our neural solver AM(ASP) against its baseline AM and MDAM.

Time Consumption - Training time is an essential facet of neural solvers. When applying ASP, there will be extra time consumption for training the data generator and evaluating the meta-payoffs in DE on top of the standard training consumption of neural solvers. All the experiments are conducted on a single GeForce RTX 3090. Under our setting, training POMO on TSP and CVRP takes 1.67 days and 2.25 days, respectively; training AM on TSP and CVRP takes 4 days and 3.3 days, respectively. When training AM for other COPs, we stop the training early once there are no further improvements, resulting in a training duration of 2 days approximately. Compared with the training cost of base solvers, training a neural solver under ASP takes slightly more time than that base solver takes on a problem scale of 50, and much less than a problem scale of 100.

5.2 Results on Generated Data

Data Generation - For TSP, We generate data by randomly sampling $x \in \mathbb{R}^2$ from the unit square, and sampling $y \in \mathbb{R}^2$ from $N(\mathbf{0}, \Sigma)$ where $\Sigma \in \mathbb{R}^{2 \times 2}$ is a diagonal matrix whose elements are sampled from $[0, \lambda]$ and $\lambda \sim U(0, 1)$. Next, a two-dimensional coordinate is generated by $z = x + y$, and we can get any scale n of TSP by performing this sampling n

TABLE 2: Our model vs baselines. The gap % is w.r.t. the best value across all methods. The bold numbers indicate base solver(ASP) achieves better performance than base solver and the underline numbers mean the best performance among all heuristic methods. We especially focus on the Avg. Gap because we care more about the performance of difference methods on several problem scales.

Method	$n = 20$		$n = 50$		$n = 100$		Avg. Gap	
	Gap	Time	Gap	Time	Gap	Time		
Concorde	0.00%	(18.50s)	0.00%	(46.38s)	0.00%	(34.52s)	0.00%	
LKH3	0.00%	(3.01s)	0.00%	(50.79s)	0.00%	(1.83m)	0.00%	
Gurobi	0.00%	(1.24s)	0.00%	(30.34s)	0.00%	(2.16m)	0.00%	
OR-Tools	1.96%	(10.47s)	3.50%	(1.07m)	4.16%	(5.11m)	3.21%	
Farthest Insertion	2.91%	(1.41s)	6.01%	(5.73s)	7.49%	(9.09s)	5.61%	
Random Insertion	5.10%	(0.99s)	8.33%	(3.24s)	10.09%	(5.85s)	8.16%	
Nearest Insertion	10.94%	(1.48s)	17.59%	(5.09s)	20.19%	(9.49s)	16.66%	
TSP	LIH(T=1000)	14.49%	(28.24s)	145.03%	(36.73s)	300.00%	(2.05m)	176.64%
	GCN(gr.)	17.82%	(17.30s)	75.92%	(18.55s)	52.92%	(1.01m)	48.37%
	GCN(bs)	16.16%	(1.03m)	74.36%	(1.32m)	48.05%	(4.97m)	46.70%
	MDAM(gr.)	0.72%	(9.61s)	12.57%	(32.36s)	13.97%	(12.06m)	9.09%
	MDAM(bs.)	0.65%	(52.18s)	5.56%	(20.95m)	12.99%	(38.87m)	5.91%
	CVAE-Opt	2.90%	(1.39m)	7.33%	(3.01m)	3.62%	(4.74m)	4.62%
	AM	5.95%	(0.02s)	65.77%	(0.04s)	53.30%	(0.12s)	41.67%
	AM(ASP)	1.81%	(0.03s)	3.98%	(0.07s)	5.60%	(0.16s)	3.79%
	POMO	0.01%	(0.45s)	0.42%	(1.43s)	2.81%	(5.67s)	1.09%
	POMO(ASP)	<u>0.09%</u>	(0.45s)	<u>0.59%</u>	(1.44s)	<u>1.67%</u>	(5.67s)	<u>0.78%</u>
CVRP	LKH3	0.00%	(4.81m)	0.00%	(8.23m)	0.00%	(16.09m)	0.00%
	Gurobi(10s)	1.74%	(11.69s)	33.08%	(12.15s)	40.44%	(12.70s)	32.38%
	Gurobi(50s)	1.39%	(51.80s)	14.93%	(53.80s)	32.58%	(53.65s)	14.87%
	Gurobi(100s)	2.78%	(1.70m)	10.20%	(1.72m)	21.54%	(1.78m)	10.82%
	RL(gr.)	42.51%	(2.72s)	14.42%	(5.04s)	47.94%	(6.12s)	39.54%
	RL(bs.)	34.84%	(6.06s)	9.95%	(28.42s)	41.57%	(35.48s)	33.67%
	MDAM(gr.)	3.48%	(3.95s)	11.95%	(6.15s)	12.49%	(18.18s)	9.31%
	MDAM(bs.)	1.74%	(9.48s)	9.19%	(24.19s)	10.45%	(1.02m)	7.13%
	CVAE-Opt	5.57%	(4.08m)	9.43%	(3.71m)	16.79%	(3.92m)	10.60%
	LoRew	29.95%	(0.34s)	84.70%	(2.64s)	152.41%	(5.77s)	85.08%
AM	5.72%	(0.02s)	11.35%	(0.06s)	18.09%	(0.11s)	11.72%	
AM(ASP)	9.48%	(0.04s)	7.73%	(0.11s)	11.27%	(0.21s)	9.49%	
POMO	0.32%	(0.04s)	1.27%	(0.14s)	3.00%	(0.51s)	1.53%	
POMO(ASP)	0.37%	(0.04s)	<u>1.26%</u>	(0.11s)	<u>2.79%</u>	(0.44s)	<u>1.47%</u>	
SDVRP	MDAM(gr.)	3.83%	(4.17s)	10.80%	(9.37s)	16.79%	(21.59s)	10.47%
	MDAM(bs.)	<u>2.43%</u>	(11.01s)	8.27%	(23.61s)	13.43%	(1.30m)	8.03%
	AM	6.20%	(0.03s)	26.79%	(0.08s)	19.56%	(0.15s)	17.52%
	AM(ASP)	13.32%	(0.05s)	8.34%	(0.13s)	11.88%	(0.26s)	11.18%
PCTSP	Gurobi	0.00%	(0.30s)	0.00%	(0.95s)	0.00%	(2.98m)	0.00%
	OR-Tools	2.20%	(11.06s)	5.33%	(2.00m)	8.33%	(6.00m)	5.30%
	ILS(python 10x)	63.23%	(3.05s)	148.05%	(4.70s)	209.78%	(5.27s)	137.94%
	MDAM(gr.)	11.76%	(41.10s)	24.73%	(1.31m)	30.07%	(1.96m)	22.19%
	MDAM(bs.)	5.88%	(2.70m)	18.81%	(4.77m)	26.09%	(6.97m)	16.93%
	AM	2.88%	(0.02s)	17.95%	(0.06s)	29.24%	(0.14s)	16.69%
AM(ASP)	12.05%	(0.03s)	10.34%	(0.08s)	11.56%	(0.18s)	11.32%	
SPCTSP	MDAM(gr.)	11.76%	(20.33s)	24.73%	(11.36s)	30.07%	(16.97s)	22.19%
	MDAM(bs.)	7.35%	(1.06m)	20.43%	(2.02m)	26.81%	(3.10m)	18.20%
	AM	3.60%	(0.02s)	15.68%	(0.06s)	33.09%	(0.13s)	17.45%
	AM(ASP)	<u>10.74%</u>	(0.04s)	<u>7.69%</u>	(0.07s)	<u>8.16%</u>	(0.16s)	<u>8.86%</u>

times. We sample 10000 normalized instances which make up 10 groups of data generated by different λ values. For

CVRP, the generation of two-dimension coordinates is same as TSP, the demands δ is discrete and sampled uniformly

from $\{1, \dots, 9\}$ and the capacity is $D^{20} = 30, D^{30} = D^{40} = D^{50} = 30, D^{60} = D^{70} = \dots = D^{100} = 50$ and the final demand is normalized to $\hat{\delta} = \frac{\delta}{D}$. The evaluation size is 128. For PCTSP and SPCTSP, the maximal length is $L^{20} = 2, L^{30} = L^{40} = L^{50} = 3, L^{60} = L^{70} = \dots = L^{100} = 4$. Then we keep the same generation setting for the prize and penalty in AM [2], the generation of two-dimension coordinates is same as TSP and the evaluation size is 1000. The overall results on problem scale of 20, 50, 100 are shown in Table 2.

Remark – It is worth mentioning the comparing scenario at the beginning: we evaluate one *base solver*(ASP) on different problem scales while the other neural solvers are evaluated with models trained on separate problem scales. That is, we use one universal neural solver to achieve better performance than several base solvers (3 in our case).

Results on TSP – We compare various baselines with several neural solvers. Firstly, the performance of neural solvers trained on uniform distribution has a huge decrease on unseen distribution. Specifically, in terms of the average gap, the performances of LIH [17], GCN [49], MDAM [48] and AM [2] are worse than the classical heuristics, e.g. Farthest Insertion and Random Insertion. It’s especially undesirable as neural solvers need extra cost for training. The performance of CVAE-Opt [50] and POMO [5] are relatively stable. For the comparison between the base solvers and our method, AM(ASP) and POMO(ASP) have a great decrease of 90.9% and 49.4% compared with AM and POMO while the time-consumption is almost no further increase¹. What’s more, POMO(ASP) achieves the best results among all solvers except for the exact methods.

Results on VRP – For CVRP, the neural solvers have dominant performance w.r.t. time-consumption compared with the classic solvers. For the solution quality, the neural solvers still suffer from the impacts of data distribution heavily except POMO [5]. For the comparison of base solvers and our method, AM(ASP) and POMO(ASP) have a 19% and 5% decrease over AM and POMO without increased time consumption. Furthermore, even compared with Gurobi (10s, 50s, 100s) [46] and OR-Tools [53] in terms of solution quality and time-consumption, POMO(ASP) achieves the best performance among all these baselines, showing the potential of neural solvers to handle more complex tasks. For SDVRP, AM(ASP) also has a 36.2% improvement compared with AM.

Results on PCTSP – Compared with classical solvers and heuristics, neural solvers still have superiority over the time-consumption. For the solution quality, AM and AM(ASP) outperform Iterated Local Search (ILS) by a large margin. Moreover, AM (ASP)’s performance is better than AM with a 32.2% decrease. Similar to the results on SPCTSP, AM(ASP)’s performance surpasses AM by 29.2%, showing a much better generalization ability for real problems.

5.3 Results on Real World Data

We show the experimental results on real datasets in Table 3–4. Note both AM and POMO are trained under the

1. The time cost of AM(ASP) is slightly larger than AM because we use more model capacity. The reasons are shown in section 6.4 and B

problem scale of 100, requiring far more training time than AM(ASP) and POMO(ASP).

TABLE 3: Results on TSPLib instances for TSP. The underlined and bold figures mean achieving better results than OR-Tools and the original base solver, respectively.

Instance	Opt.	OR-Tools	AM	AM(ASP)	POMO	POMO(ASP)
pr226	80,369	82,968	86,200	83,570	81,903	83,117
ts225	126,643	128,564	143,994	140,783	134,184	138,846
kroD100	21,294	21,636	21,913	21,817	21,878	21,508
eil51	426	436	434	438	428	429
kroA100	21,282	21,448	23,500	21,573	21,691	21,332
pr264	49,135	51,954	60,952	57,398	51,812	55,643
pr152	73,682	75,834	76,984	77,008	<u>74,088</u>	<u>75,086</u>
rat99	1,211	1,232	1,329	1,298	1,273	1,221
kroA150	26,524	32,474	29,674	27,799	27,087	26,982
lin105	14,382	14,824	16,423	14,640	14,853	14,531
pr124	59,030	62,519	62,350	59,981	59,385	59,399
st70	675	683	701	677	677	682
a280	2,586	2,713	3,127	2,913	2,844	2,891
rd100	7,910	8,189	8,191	8,316	7,917	7,923
pr136	96,772	102,213	103,878	100,927	<u>98,183</u>	<u>99,671</u>
pr76	108,159	111,104	109,958	109,123	<u>108,280</u>	<u>108,328</u>
kroA200	29,368	29,714	33,033	31,673	29,946	30,313
kroB200	29,437	30,516	32,501	31,309	30,999	30,499
pr107	44,303	45,072	48,115	47,321	44,856	45,222
kroB150	26,130	27,572	27,837	26,925	26,680	26,441
u159	42,080	45,778	45,302	43,178	42,716	42,768
berlin52	7,542	7,945	8,483	7,593	7,548	7,544
rat195	2,323	2,389	2,855	2,699	2,506	2,527
d198	15,780	15,963	24,324	18,482	19,864	17,737
eil101	642	664	663	659	643	643
pr144	58,537	59,286	62,038	59,702	59,173	59,173
pr299	48,191	48,447	60,506	56,955	52,807	53,213
kroC100	20,750	21,583	22,491	20,896	20,906	20,753
tsp225	3,859	4,046	4,563	4,361	4,146	4,180
eil76	538	561	562	555	549	553
kroB100	22,141	23,006	23,293	22,923	22,336	22,376
kroE100	22,068	22,598	23,311	22,733	22,415	22,183
ch150	6,532	6,729	6,851	6,756	6,590	6,609
bier127	118,282	137,893	128,308	121,687	<u>124,391</u>	<u>122,874</u>
ch130	6,110	6,284	6,452	6,218	<u>6,137</u>	<u>6,137</u>
Avg. Gap (%)	0	4.19	10.69	5.62	<u>3.37</u>	3.23

Results on TSP – We further verify the neural solvers trained by ASP in TSPLib [11]. As shown in Table 3, AM(ASP) outperforms AM in almost all instances with an decrease of 5% on the average optimality gap. Specifically, for several instances: lin105, st70, pr136, kroB150, berlin52, eil101, kroC100, eil76 and ch130, ASP can help AM surpass OR-Tools. For POMO [5], ASP can still improve it to some extent. What’s more, POMO(ASP) outperforms all listed methods and has a better average optimality gap. The above results can show that neural solvers trained via ASP can handle difficult and real instances by generalizing to complex distributions and a set of problem scales.

Results on CVRP – We compare the solution qualities of the neural solvers trained by ASP with base solvers AM [2], POMO [5], and OR-Tools on the real-world instances from CVRPLib [12] B, E, F, and X, covering the problem scales range from 22 to 181. In these real instances, AM(ASP) has better performance than AM in terms of the average optimality gap. The neural solver POMO(ASP) outperforms POMO [5] on approximately 70% (37 out of 53) of the selected CVRPLib instances and achieves a better average gap 3.32% than baseline 6.10%. Additionally, POMO(ASP) also achieves better performance than OR-tools on 47 out of 53 instances and has a decrease of 65% in terms of the average gap.

Based on the results on the real benchmark, we can conclude neural solvers trained after ASP can improve the generalization ability observably with the same model capacity and far less training time.

TABLE 4: Results on CVRplib Instances for CVRP. The underlined and bold numbers indicate better results than OR-Tools and the original base solver, respectively.

Instance	Opt.	OR-Tools	AM	AM(ASP)	POMO	POMO(ASP)
B-n52-k7	747	759	806	850	753	<u>755</u>
B-n66-k9	1,316	1,390	1,437	1,418	1,335	1,331
B-n68-k9	1,272	1,389	1,316	1,419	1,301	<u>1,313</u>
B-n45-k6	678	769	<u>748</u>	735	717	689
B-n50-k8	1,312	1,335	1,378	1,358	1,329	1,359
B-n57-k9	1,598	1,689	1,674	1,647	<u>1,607</u>	1,617
B-n51-k7	1,032	1,150	<u>1,034</u>	1,165	1,030	1,025
B-n50-k7	741	748	788	857	748	764
B-n39-k5	549	590	577	645	556	554
B-n31-k5	672	677	717	702	729	681
B-n63-k10	1,496	1,627	1,633	1,597	1,540	1,579
B-n64-k9	861	1,105	1,010	<u>915</u>	910	<u>924</u>
B-n67-k10	1,032	1,105	<u>1,144</u>	1,146	1,101	1,070
B-n41-k6	829	861	862	940	<u>843</u>	842
B-n44-k7	909	948	1,030	993	934	950
B-n56-k7	707	779	742	766	715	721
B-n34-k5	788	798	825	864	803	796
B-n35-k5	955	996	1,097	975	976	974
B-n45-k5	751	804	864	812	763	762
B-n38-k6	805	881	847	852	820	817
B-n78-k10	1,221	1,299	1,336	1,313	1,255	1,265
B-n43-k6	742	771	830	770	763	747
E-n22-k4	375	375	441	408	417	375
E-n23-k3	569	570	620	620	702	572
E-n33-k4	835	937	855	956	870	839
E-n51-k5	521	587	582	572	553	532
E-n76-k7	682	740	718	764	702	700
E-n76-k8	735	824	790	822	750	747
E-n76-k10	830	992	880	926	853	851
E-n76-k14	1021	1,586	1,110	1,120	1,051	1,042
E-n101-k8	815	993	<u>863</u>	<u>900</u>	<u>845</u>	845
E-n101-k14	1,067	1,238	<u>1,119</u>	1,242	1,118	1,117
F-n45-k4	724	733	784	758	761	<u>725</u>
F-n72-k4	237	315	308	267	260	266
F-n135-k7	1,162	1,427	1,592	1,398	1,284	1,334
X-n101-k25	27,591	29,405	30,140	29,783	35,824	29,137
X-n106-k14	26,362	27,343	27,661	28,676	27,994	27,304
X-n110-k13	14,971	16,149	15,896	16,367	15,132	15,366
X-n115-k10	12,747	13,320	15,155	14,635	13,429	13,885
X-n120-k6	13,332	14,242	14,709	16,167	14,137	13,805
X-n125-k30	55,539	58,665	61,176	59,603	68,326	58,317
X-n129-k18	28,940	31,361	30,900	30,560	29,450	29,469
X-n134-k13	10,916	13,275	<u>12,643</u>	12,108	11,421	11,303
X-n139-k10	13,590	15,223	<u>15,042</u>	14,873	<u>13,982</u>	13,972
X-n143-k7	15,700	17,470	17,661	17,450	16,157	16,379
X-n148-k46	43,448	46,836	52,201	47,545	54,698	45,456
X-n153-k22	21,220	22,919	25,832	24,449	23,581	23,317
X-n157-k13	16,876	17,309	18,923	18,374	17,424	17,371
X-n162-k11	14,138	15,030	14,880	15,786	15,022	14,814
X-n167-k10	20,557	22,477	<u>22,677</u>	22,478	21,454	21,113
X-n172-k51	45,607	50,505	55,098	50,044	60,646	48,850
X-n176-k26	47,812	52,111	56,449	56,582	53,150	52,012
X-n181-k23	25,569	26,321	27,114	26,951	28,176	26,208
Avg. Gap (%)	0	9.52	10.74	9.88	6.10	3.32

6 DISCUSSION

In this section, we conduct various ablation studies about essential training details: training paradigm, task selection strategy, performance threshold, model capacity, and training sample size. Based on these results, we provide a comprehensive view of the ASP framework and some training insights for neural solvers for future work. For all the ablation studies, we keep the other settings the same except for the factors we focus on and run them under 5 random generated seeds.

6.1 Comparison Between Different Training Paradigm

To verify the validity of the ASP framework, we train POMO and AM with mixed problem scales 20, 40, 60, 80, and 100 on uniform distribution, which we denote as ‘‘Uniformly Train’’. As demonstrated in Fig. 2, POMO under uniform training can achieve competitive performance compared with the ASP framework. However, the performances of AM by uniform training are quite worse and the training even fails for TSP and CVRP. This observation indicates

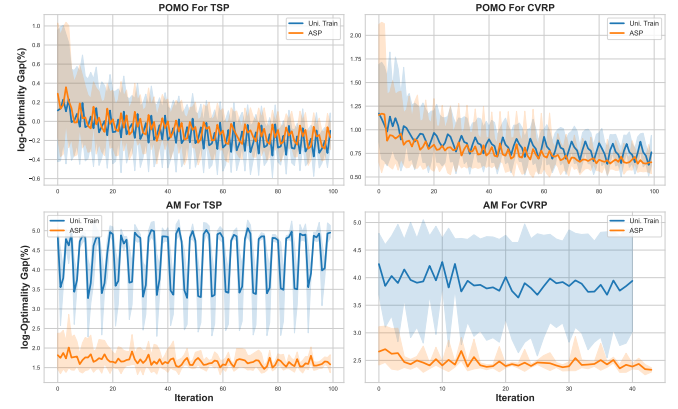


Fig. 2: Comparisons of Uniformly Train and ASP. Uniformly train means training all problem scales at the same time and training samples of each problem scale are equal. With Uniformly Train, POMO can achieve competitive results with ASP on TSP and a little worse performance on CVRP. However for AM, the training of Uniformly Train fails on TSP and the performance is poor on CVRP, while ASP can gain consistent improvement for POMO and AM on both TSP and CVRP.

that neural solvers do not consistently benefit from a naive training procedure by mixing different types of problem instances. However, the ASP framework shows excellent transferability and thus fits multiple neural solvers and COPs.

6.2 Influence of Task Selection Strategy

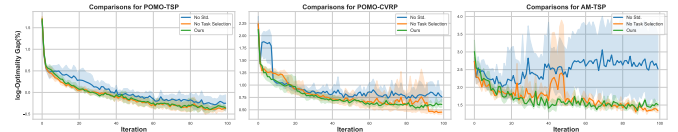


Fig. 3: Comparisons of the different training strategies. No Task Selection, No Std. and Ours in the legend mean using uniform strategy, $\lambda = 1$ and $\lambda = 0.5$ in Eq. 12 during training. There are cases when the training fails for Task Selection and No Std, e.g. training POMO for CVRP and training AM for TSP. However, ASP shows training stability for all demonstrated cases.

We propose the task selection strategy in Eq. 12:

$$p_i^t \propto \lambda p_i^1 + (1 - \lambda) p_i^2, \lambda \in [0, 1]$$

which receives the information from target distribution to guide the training process. Two naive choices for the task selection strategy are (1) uniform, meaning no preference for specific tasks, and (2) $\lambda = 1$, a short-sighted choice to emphasize current performance. Compared with these candidates, our strategy evidently has superiority by taking both the need for improvement and stability into consideration. Experimental results show that these two candidate strategies may fail the training in some cases. As shown in Fig. 3, we evaluate the neural solvers during the training process on the evaluation dataset: Base solver-COP means

we train base solvers under the ASP framework on a specific COP with different task selection strategies, "No Std.", "No Task Selection" and "Ours" mean the case of $\lambda = 1$, uniform strategy and $\lambda = 0.5$, respectively. Three subfigures show that these three strategies may perform well in some cases, e.g. in the case of POMO-TSP in the leftmost subfigure. However, "No Std" and "No Tasks Selection" show the instability under different random seeds when training POMO-CVRP and even fail the training for AM-TSP because the shortsighted strategy of only considering improvement and uniform strategy can mislead the training. However, ASP performs stably and works well for all neural solvers and COPs under different random seeds.

6.3 Influence of Performance Threshold

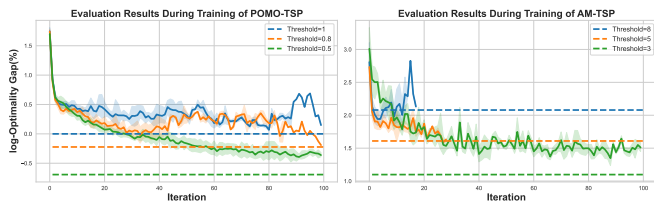


Fig. 4: Comparisons of different thresholds for POMO-TSP and AM-TSP w.r.t. the optimality gap (%) in the log-scale. A lower standard (larger threshold here) will lead to the early stopping of training, for example, AM-TSP achieves the threshold of 8 at a very early iteration. What’s more, proper setting of the threshold can improve the performance, for example, POMO-TSP can gain better performance with a threshold of 0.5 than that of 0.8, even though the threshold of 0.5 is not reached eventually.

The appropriate threshold is beneficial to the performance a lot. Excessive expectations can lead to indecision while low expectations would cause slacking off. Fig. 4 shows the evaluation curves of neural solvers during the training phase under different performance thresholds. For POMO-TSP, we select three performance thresholds: 1, 0.8, 0.5 and keep the other settings the same; for AM-TSP, we select threshold=8, 5, 3 for comparisons. On one hand, if the performance threshold is too large, the training process of the ASP framework will stop in advance, resulting in fewer iterations of the PSA procedure (Algorithm 2). For example, when we set threshold=8 for AM-TSP, the training process stops at very early iteration. On the other hand, if the threshold is too harsh, the neural solver would never achieve the expectation due to its limits, e.g. model capacity, training sample size, etc. For instance, threshold=0.5 for POMO-TSP and threshold=3 for AM-TSP are so rigorous that they can’t achieve their goal at the end of training. However, harsh thresholds still promote the neural solver to gain better performance. For instance, even though POMO-TSP is not able to achieve the threshold of 0.5, it can still have better performance on that of training with threshold=0.8.

An obvious guidance of designing the threshold is the performance of the original neural solver which is fixed throughout the whole training process. We believe that a dynamic threshold adjustment procedure will help a lot

because the neural solver has different performances on different problem scales.

6.4 Influence of Model Capacity

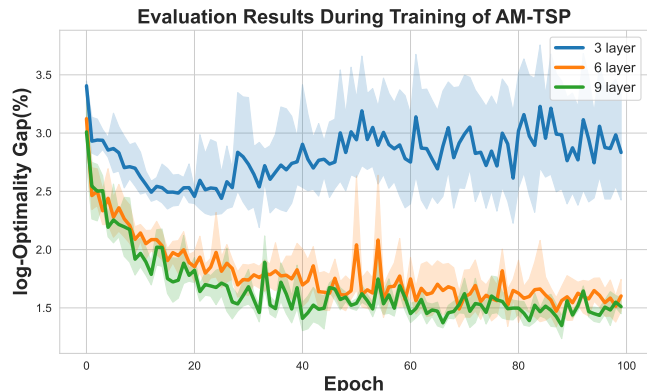


Fig. 5: Evaluation results of AM-TSP with different encoder layers w.r.t. optimality gap (%) in the log-scale. We can see that a small model capacity will lead to worse performance and even the failure of training.

During the whole training process, we are about to handle a set of problem scales and more complicated distributions which is much harder than solely focusing on a specific problem scale and uniform distribution. When dealing with harder tasks, model capacity is a significant facet impacting the final results, as shown in Fig. 5. We can see that AM with 3 encoder layers fails the training while AM with 6 and 9 layers can converge stably, which in turn verifies our assumption. What’s more, AM-TSP with 9 encoder layers can obtain better results than that with 6 layers, meaning better performance comes with a larger capacity.

6.5 Influence of Training Sample Size

The training sample size is also an important factor influencing the final performance. We show the ablation results for POMO-TSP and AM-TSP in Fig. 6 and the performance threshold is 0.5 for POMO-TSP and 3 for AM-TSP. In the legend of this figure, "Normal" means the sample size N in the default setting of our training, "Small" and "Tiny" mean the sample size of $\frac{N}{10}$ and $\frac{N}{100}$, respectively. The same threshold can act as a standard to make the comparison clear and fair. It’s obvious that a larger sample size remarkably contributes to the final results on the convergence rate and stopping iterations. However, a larger sample size also implies more computational burden. The right bar plot in Fig. 6 shows the average training time consumption for different sample sizes in the log-hour scale, so we need to balance this trade-off in realistic cases.

6.6 Effects of ASP on the Landscape

There has been a widely-discussed claim whether the shape of the metric landscape is related to the generalization ability [54], [55], [56], [57]. Some researchers think that "sharp"

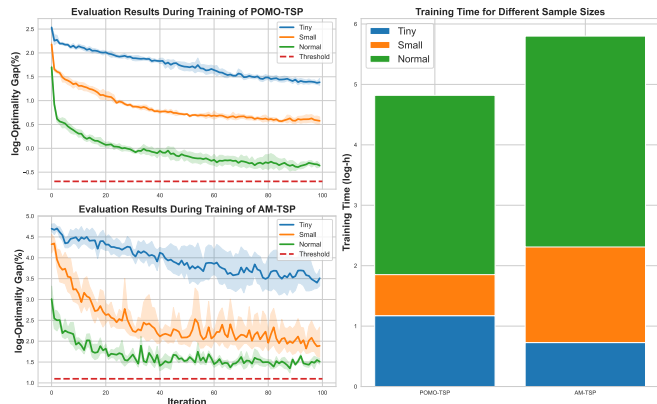


Fig. 6: Comparisons of the different sample size. Normal, Small, and Tiny mean the different scales of sample size. The Normal sample size is 10 times larger than Small and The small sample size is 10 times larger than Tiny. The left subfigures show the evaluation results during training and the right one shows the average training time of different random seeds in the log-scale of hours.

landscape would have poor generalization [58], [59] due to the large batch size during training, but some others propose specialized training methods to achieve good generalization ability with large batch size [59]. In this part, we dive into the generalization ability of AM and POMO by visualizing the return landscape and discussing some insights. We leave specific visualization configurations and further visualization results in Appendix F.

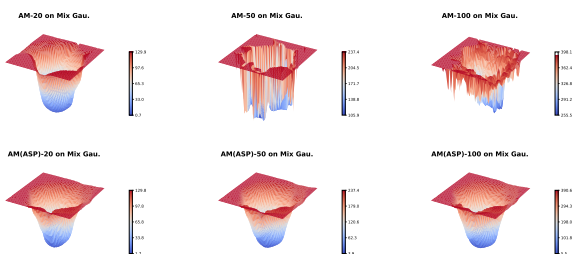


Fig. 7: The landscape of optimality gap(%) for AM testing on mixed gaussian distribution.

Discussion for AM. We visualize the landscape of optimality gap(%) for AM and AM(ASP) on the mixed gaussian distribution in Fig. 7. Under the same perturbation settings on the parameter, we can see that as the problem scale grows, the landscape is more steep or sharp. For example, the ranges of optimality gap(%) for AM(ASP) on TSP20, TSP50, and TSP100 are 1.7% ~ 129.8%, 3.9% ~ 237.4% and 5.5% ~ 390.6%, respectively, showing that the bigger the problem scale is, the wider the range becomes. What’s more, sharper minima means it’s more difficult to achieve [60], so we need to pay more attention to the optimization level or spend more time on training. Combining the prior knowledge that larger-scale COPs are harder than smaller ones, we can conclude that large-scale COPs (harder tasks) are more difficult to train than small-scale COPs (easier tasks), which is accordant with the common practice: we always need

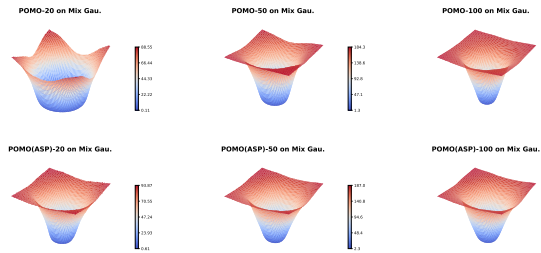


Fig. 8: The landscape of optimality gap(%) for POMO testing on mixed gaussian distribution.

more training time and get worse performance on large-scale COPs than those on small-scale COPs. Interestingly, the optimization level’s observation also coincides with the rule of starting from easy tasks in curriculum training: what curriculum training does is to start from a “wide minima” to a “sharp minima”.

As for the comparison between AM and AM(ASP), we can see that the landscapes of AM on TSP50 and TSP100 are quite messy, while that on TSP20 is relatively smooth, which aligns with the results in Table 2 and 6 that AM performs well on TSP20 but poorly on TSP50 and TSP100. However, all the landscapes obtained from AM(ASP) share the smoothness for all problem scales.

Discussion for POMO. We visualize the landscape of optimality gap(%) for POMO and POMO(ASP) on the mixed gaussian distribution in Fig. 8. The relationship between the generalization ability on the problem scale and the curvature of the landscape for POMO shares the same rule: a bigger problem scale has a sharper landscape of optimality gap. Moreover, unlike AM, POMO has a smooth landscape on all problem scales like POMO(ASP), which is accordant to the results in Table 2 and 6. According to the shape of the landscape, we may say that POMO is a more powerful neural solver than AM in some sense.

7 CONCLUSION

Inspired by the framework of PSRO and Adaptive Staircase, in this paper, we propose the game-theoretic and curriculum learning-based solution, ASP, which for the first time improves the generalization ability from multiple aspects for the RL-based neural solvers on COPs. We evaluate our method on several typical COPs and employ different neural solvers. On both randomly-generated and real-world benchmarks, we show that the neural solver trained under our framework demonstrates impressive generalization performance when compared to a series of baselines. As such, a neural solver trained via ASP may avoid over-fitting and consistently achieve robust performance even on the distribution and problem scales it has never trained, which has never been accomplished in existing neural solvers. Therefore, we rationally believe that ASP can lead to the first step in applying neural solvers to industrial use.

REFERENCES

- [1] E. Khalil, H. Dai, Y. Zhang, B. Dilkina, and L. Song, “Learning combinatorial optimization algorithms over graphs,” *Advances in neural information processing systems*, 2017.

- [2] W. Kool, H. van Hoof, and M. Welling, "Attention, learn to solve routing problems!," in *7th International Conference on Learning Representations, ICLR 2019, New Orleans, LA, USA, May 6-9, 2019*, OpenReview.net, 2019.
- [3] Y. Wu, W. Song, Z. Cao, J. Zhang, and A. Lim, "Learning improvement heuristics for solving routing problems.," *IEEE Transactions on Neural Networks and Learning Systems*, 2021.
- [4] W. Kool, H. van Hoof, J. A. S. Gromicho, and M. Welling, "Deep policy dynamic programming for vehicle routing problems," in *Integration of Constraint Programming, Artificial Intelligence, and Operations Research - 19th International Conference, CPAIOR 2022, Los Angeles, CA, USA, June 20-23, 2022, Proceedings* (P. Schaus, ed.), vol. 13292 of *Lecture Notes in Computer Science*, pp. 190–213, Springer, 2022.
- [5] Y.-D. Kwon, J. Choo, B. Kim, I. Yoon, Y. Gwon, and S. Min, "Pomo: Policy optimization with multiple optima for reinforcement learning," *Advances in Neural Information Processing Systems*, vol. 33, pp. 21188–21198, 2020.
- [6] C. Wang, Y. Yang, O. Slumbers, C. Han, T. Guo, H. Zhang, and J. Wang, "A game-theoretic approach for improving generalization ability of tsp solvers," *arXiv preprint arXiv:2110.15105*, 2021.
- [7] Z. Zhang, Z. Zhang, X. Wang, and W. Zhu, "Learning to solve travelling salesman problem with hardness-adaptive curriculum," in *AAAI*, 2022.
- [8] M. Lisicki, A. Afkanpour, and G. W. Taylor, "Evaluating curriculum learning strategies in neural combinatorial optimization," *arXiv preprint arXiv:2011.06188*, 2020.
- [9] B. Treutwein, "Adaptive psychophysical procedures," *Vision research*, vol. 35, no. 17, pp. 2503–2522, 1995.
- [10] L. Dinh, J. Sohl-Dickstein, and S. Bengio, "Density estimation using real NVP," in *5th International Conference on Learning Representations, ICLR 2017, Toulon, France, April 24-26, 2017, Conference Track Proceedings*, OpenReview.net, 2017.
- [11] G. Reinelt, "TspLib—a traveling salesman problem library," *ORSA journal on computing*, vol. 3, no. 4, pp. 376–384, 1991.
- [12] E. Uchoa, D. Pecin, A. Pessoa, M. Poggi, T. Vidal, and A. Subramanian, "New benchmark instances for the capacitated vehicle routing problem," *European Journal of Operational Research*, vol. 257, no. 3, pp. 845–858, 2017.
- [13] O. Vinyals, M. Fortunato, and N. Jaitly, "Pointer networks," in *Advances in Neural Information Processing Systems 28: Annual Conference on Neural Information Processing Systems 2015, December 7-12, 2015, Montreal, Quebec, Canada* (C. Cortes, N. D. Lawrence, D. D. Lee, M. Sugiyama, and R. Garnett, eds.), pp. 2692–2700, 2015.
- [14] I. Bello, H. Pham, Q. V. Le, M. Norouzi, and S. Bengio, "Neural combinatorial optimization with reinforcement learning," in *5th International Conference on Learning Representations, ICLR 2017, Toulon, France, April 24-26, 2017, Workshop Track Proceedings*, OpenReview.net, 2017.
- [15] A. Vaswani, N. Shazeer, N. Parmar, J. Uszkoreit, L. Jones, A. N. Gomez, L. Kaiser, and I. Polosukhin, "Attention is all you need," in *Advances in Neural Information Processing Systems 30: Annual Conference on Neural Information Processing Systems 2017, December 4-9, 2017, Long Beach, CA, USA* (I. Guyon, U. von Luxburg, S. Bengio, H. M. Wallach, R. Fergus, S. V. N. Vishwanathan, and R. Garnett, eds.), pp. 5998–6008, 2017.
- [16] P. Veličković, G. Cucurull, A. Casanova, A. Romero, P. Lio, and Y. Bengio, "Graph attention networks," *arXiv preprint arXiv:1710.10903*, 2017.
- [17] H. Lu, X. Zhang, and S. Yang, "A learning-based iterative method for solving vehicle routing problems," in *8th International Conference on Learning Representations, ICLR 2020, Addis Ababa, Ethiopia, April 26-30, 2020*, OpenReview.net, 2020.
- [18] Z. Fu, K. Qiu, and H. Zha, "Generalize a small pre-trained model to arbitrarily large TSP instances," in *Thirty-Fifth AAAI Conference on Artificial Intelligence, AAAI 2021, Thirty-Third Conference on Innovative Applications of Artificial Intelligence, IAAI 2021, The Eleventh Symposium on Educational Advances in Artificial Intelligence, EAAI 2021, Virtual Event, February 2-9, 2021*, pp. 7474–7482, AAAI Press, 2021.
- [19] F. Agostinelli, S. McAleer, A. Shmakov, and P. Baldi, "Solving the rubik's cube with deep reinforcement learning and search," *Nature Machine Intelligence*, vol. 1, no. 8, pp. 356–363, 2019.
- [20] F. Agostinelli, A. Shmakov, S. McAleer, R. Fox, and P. Baldi, "A* search without expansions: Learning heuristic functions with deep q-networks," *arXiv preprint arXiv:2102.04518*, 2021.
- [21] Y. Bengio, A. Lodi, and A. Prouvost, "Machine learning for combinatorial optimization: a methodological tour d'horizon," *European Journal of Operational Research*, 2020.
- [22] K. Smith-Miles and S. Bowly, "Generating new test instances by evolving in instance space," *Computers & Operations Research*, vol. 63, pp. 102–113, 2015.
- [23] G. Zuzic, D. Wang, A. Mehta, and D. Sivakumar, "Learning robust algorithms for online allocation problems using adversarial training," *arXiv preprint arXiv:2010.08418*, 2020.
- [24] S. Liu, K. Tang, and X. Yao, "Generative adversarial construction of parallel portfolios," *IEEE transactions on cybernetics*, 2020.
- [25] I. Goodfellow, J. Pouget-Abadie, M. Mirza, B. Xu, D. Warde-Farley, S. Ozair, A. Courville, and Y. Bengio, "Generative adversarial nets," *Advances in neural information processing systems*, vol. 27, 2014.
- [26] M. Lanctot, V. F. Zambaldi, A. Gruslys, A. Lazaridou, K. Tuyls, J. Pérolat, D. Silver, and T. Graepel, "A unified game-theoretic approach to multiagent reinforcement learning," in *Advances in Neural Information Processing Systems 30: Annual Conference on Neural Information Processing Systems 2017, December 4-9, 2017, Long Beach, CA, USA* (I. Guyon, U. von Luxburg, S. Bengio, H. M. Wallach, R. Fergus, S. V. N. Vishwanathan, and R. Garnett, eds.), pp. 4190–4203, 2017.
- [27] S. McAleer, K. Wang, M. Lanctot, J. Lanier, P. Baldi, and R. Fox, "Anytime optimal psro for two-player zero-sum games," *arXiv preprint arXiv:2201.07700*, 2022.
- [28] N. Perez-Nieves, Y. Yang, O. Slumbers, D. H. Mguni, Y. Wen, and J. Wang, "Modelling behavioural diversity for learning in open-ended games," in *International Conference on Machine Learning*, pp. 8514–8524, PMLR, 2021.
- [29] S. McAleer, J. Lanier, K. Wang, P. Baldi, R. Fox, and T. Sandholm, "Self-play psro: Toward optimal populations in two-player zero-sum games," *arXiv preprint arXiv:2207.06541*, 2022.
- [30] J. Perolat, B. De Vylder, D. Hennes, E. Tarassov, F. Strub, V. de Boer, P. Muller, J. T. Connor, N. Burch, T. Anthony, et al., "Mastering the game of stratego with model-free multiagent reinforcement learning," *Science*, vol. 378, no. 6623, pp. 990–996, 2022.
- [31] H. Fu, W. Liu, S. Wu, Y. Wang, T. Yang, K. Li, J. Xing, B. Li, B. Ma, Q. Fu, et al., "Actor-critic policy optimization in a large-scale imperfect-information game," in *International Conference on Learning Representations*, 2021.
- [32] S. McAleer, G. Farina, M. Lanctot, and T. Sandholm, "Escher: Eschewing importance sampling in games by computing a history value function to estimate regret," *arXiv preprint arXiv:2206.04122*, 2022.
- [33] Y. Bengio, J. Louradour, R. Collobert, and J. Weston, "Curriculum learning," in *Proceedings of the 26th annual international conference on machine learning*, pp. 41–48, 2009.
- [34] A. Pentina, V. Sharmanska, and C. H. Lampert, "Curriculum learning of multiple tasks," *2015 IEEE Conference on Computer Vision and Pattern Recognition (CVPR)*, pp. 5492–5500, 2015.
- [35] S. Guo, W. Huang, H. Zhang, C. Zhuang, D. Dong, M. R. Scott, and D. Huang, "Curriculumnet: Weakly supervised learning from large-scale web images," in *Proceedings of the European conference on computer vision (ECCV)*, pp. 135–150, 2018.
- [36] Y. Tay, S. Wang, A. T. Luu, J. Fu, M. C. Phan, X. Yuan, J. Rao, S. C. Hui, and A. Zhang, "Simple and effective curriculum pointer-generator networks for reading comprehension over long narratives," in *Proceedings of the 57th Conference of the Association for Computational Linguistics, ACL 2019, Florence, Italy, July 28- August 2, 2019, Volume 1: Long Papers* (A. Korhonen, D. R. Traum, and L. Màrquez, eds.), pp. 4922–4931, Association for Computational Linguistics, 2019.
- [37] E. A. Platanios, O. Stretcu, G. Neubig, B. Póczos, and T. M. Mitchell, "Competence-based curriculum learning for neural machine translation," in *Proceedings of the 2019 Conference of the North American Chapter of the Association for Computational Linguistics: Human Language Technologies, NAACL-HLT 2019, Minneapolis, MN, USA, June 2-7, 2019, Volume 1 (Long and Short Papers)* (J. Burstein, C. Doran, and T. Solorio, eds.), pp. 1162–1172, Association for Computational Linguistics, 2019.
- [38] C. Florensa, D. Held, M. Wulfmeier, M. Zhang, and P. Abbeel, "Reverse curriculum generation for reinforcement learning," in *Conference on robot learning*, pp. 482–495, PMLR, 2017.
- [39] Z. Ren, D. Dong, H. Li, and C. Chen, "Self-paced prioritized curriculum learning with coverage penalty in deep reinforcement

- learning,” *IEEE transactions on neural networks and learning systems*, vol. 29, no. 6, pp. 2216–2226, 2018.
- [40] S. Narvekar, B. Peng, M. Leonetti, J. Sinapov, M. E. Taylor, and P. Stone, “Curriculum learning for reinforcement learning domains: A framework and survey,” *J. Mach. Learn. Res.*, vol. 21, pp. 181:1–181:50, 2020.
- [41] R. Portelas, C. Colas, L. Weng, K. Hofmann, and P.-Y. Oudeyer, “Automatic curriculum learning for deep rl: A short survey,” in *IJCAI*, 2020.
- [42] H. Y. Huang, D. Ye, L. Shen, and W. Liu, “Curriculum-based asymmetric multi-task reinforcement learning,” *ArXiv*, vol. abs/2211.03352, 2022.
- [43] P. Toth and D. Vigo, *Vehicle routing: problems, methods, and applications*. SIAM, 2014.
- [44] E. Balas, “The prize collecting traveling salesman problem,” *Networks*, vol. 19, no. 6, pp. 621–636, 1989.
- [45] D. P. Kingma and J. Ba, “Adam: A method for stochastic optimization,” in *3rd International Conference on Learning Representations, ICLR 2015, San Diego, CA, USA, May 7-9, 2015, Conference Track Proceedings* (Y. Bengio and Y. LeCun, eds.), 2015.
- [46] Gurobi Optimization, LLC, “Gurobi Optimizer Reference Manual,” 2021.
- [47] K. Helsgaun, “An extension of the lin-kernighan-helsgaun tsp solver for constrained traveling salesman and vehicle routing problems,” *Roskilde: Roskilde University*, 2017.
- [48] L. Xin, W. Song, Z. Cao, and J. Zhang, “Multi-decoder attention model with embedding glimpse for solving vehicle routing problems,” in *Proceedings of the AAAI Conference on Artificial Intelligence*, vol. 35, pp. 12042–12049, 2021.
- [49] C. K. Joshi, T. Laurent, and X. Bresson, “An efficient graph convolutional network technique for the travelling salesman problem,” *arXiv preprint arXiv:1906.01227*, 2019.
- [50] A. Hottung, B. Bhandari, and K. Tierney, “Learning a latent search space for routing problems using variational autoencoders,” in *International Conference on Learning Representations*, 2020.
- [51] M. Nazari, A. Oroojlooy, L. V. Snyder, and M. Takác, “Reinforcement learning for solving the vehicle routing problem,” in *Advances in Neural Information Processing Systems 31: Annual Conference on Neural Information Processing Systems 2018, NeurIPS 2018, December 3-8, 2018, Montréal, Canada* (S. Bengio, H. M. Wallach, H. Larochelle, K. Grauman, N. Cesa-Bianchi, and R. Garnett, eds.), pp. 9861–9871, 2018.
- [52] X. Chen and Y. Tian, “Learning to perform local rewriting for combinatorial optimization,” *Advances in Neural Information Processing Systems*, vol. 32, 2019.
- [53] L. Perron and V. Furnon, “Or-tools.”
- [54] L. Dinh, R. Pascanu, S. Bengio, and Y. Bengio, “Sharp minima can generalize for deep nets,” in *International Conference on Machine Learning*, pp. 1019–1028, PMLR, 2017.
- [55] N. S. Keskar, D. Mudigere, J. Nocedal, M. Smelyanskiy, and P. T. P. Tang, “On large-batch training for deep learning: Generalization gap and sharp minima,” in *5th International Conference on Learning Representations, ICLR 2017, Toulon, France, April 24-26, 2017, Conference Track Proceedings*, OpenReview.net, 2017.
- [56] N. S. Keskar, D. Mudigere, J. Nocedal, M. Smelyanskiy, and P. T. P. Tang, “On large-batch training for deep learning: Generalization gap and sharp minima,” in *5th International Conference on Learning Representations, ICLR 2017, Toulon, France, April 24-26, 2017, Conference Track Proceedings*, OpenReview.net, 2017.
- [57] X. Chen and C.-J. Hsieh, “Stabilizing differentiable architecture search via perturbation-based regularization,” in *International conference on machine learning*, pp. 1554–1565, PMLR, 2020.
- [58] P. Chaudhari, A. Choromanska, S. Soatto, Y. LeCun, C. Baldassi, C. Borgs, J. Chayes, L. Sagun, and R. Zecchina, “Entropy-sgd: Biasing gradient descent into wide valleys,” *Journal of Statistical Mechanics: Theory and Experiment*, vol. 2019, no. 12, p. 124018, 2019.
- [59] S. Hochreiter and J. Schmidhuber, “Flat minima,” *Neural computation*, vol. 9, no. 1, pp. 1–42, 1997.
- [60] H. Li, Z. Xu, G. Taylor, C. Studer, and T. Goldstein, “Visualizing the loss landscape of neural nets,” *Advances in neural information processing systems*, vol. 31, 2018.

ACKNOWLEDGMENTS

This work is supported in part by the National Science and Technology Innovation 2030 – Major program of “New generation of artificial intelligence” (No. 2022ZD0116408).

APPENDIX A ORACLE TRAINING

In the algorithm 1, we need to train two oracles: S' and $P'_{\mathcal{I}^n}$ as a new policy to be added to the corresponding policy set. Here we will provide a specific derivation about the gradient for training the oracle.

Taken the formula from Eq. 5, the gradient is apparent to get:

$$\begin{aligned} \nabla_{\theta} L_{SS}(\theta) &= \nabla_{\theta} \mathbf{E}_{\mathbf{P}_{\mathcal{I}^n} \sim \sigma_{DG}} \mathbf{E}_{\mathcal{I}^n \sim \mathbf{P}_{\mathcal{I}^n}} g(S_{\theta}, \mathcal{I}^n, \text{Oracle}) \\ &= \mathbf{E}_{\mathbf{P}_{\mathcal{I}^n} \sim \sigma_{DG}} \mathbf{E}_{\mathcal{I}^n \sim \mathbf{P}_{\mathcal{I}^n}} \nabla_{\theta} g(S_{\theta}, \mathcal{I}^n, \text{Oracle}) \\ &= \mathbf{E}_{\mathbf{P}_{\mathcal{I}^n} \sim \sigma_{DG}} \mathbf{E}_{\mathcal{I}^n \sim \mathbf{P}_{\mathcal{I}^n}} \frac{\nabla_{\theta} S_{\theta}(\mathcal{I}^n)}{\text{Oracle}(\mathcal{I})}. \end{aligned} \quad (13)$$

Also for Eq. 8, the computation of this gradient is:

$$\begin{aligned} \nabla_{\gamma} L_{DG}(\gamma) &= \mathbf{E}_{S \sim \sigma_{SS}} \nabla_{\gamma} \mathbf{E}_{\mathcal{I}^n \sim \mathbf{P}_{\mathcal{I}^n, \gamma}} g(S, \mathcal{I}^n, \text{Oracle}) \\ &= \mathbf{E}_{S \sim \sigma_{SS}} \int_{\mathcal{I}} \nabla_{\gamma} \mathbf{P}_{\mathcal{I}^n, \gamma}(\mathcal{I}) g(S, \mathcal{I}, \text{Oracle}) d\mathcal{I} \\ &= \mathbf{E}_{S \sim \sigma_{SS}} \int_{\mathcal{I}} \mathbf{P}_{\mathcal{I}^n, \gamma}(\mathcal{I}) \frac{\nabla_{\gamma} \mathbf{P}_{\mathcal{I}^n, \gamma}(\mathcal{I})}{\mathbf{P}_{\mathcal{I}^n, \gamma}(\mathcal{I})} g(S, \mathcal{I}, \text{Oracle}) d\mathcal{I} \\ &= \mathbf{E}_{S \sim \sigma_{SS}} \mathbf{E}_{\mathcal{I} \sim \mathbf{P}_{\mathcal{I}, \gamma}} \nabla_{\gamma} \log \mathbf{P}_{\mathcal{I}^n, \gamma}(\mathcal{I}) g(S, \mathcal{I}, \text{Oracle}). \end{aligned} \quad (14)$$

APPENDIX B TRAINING DETAILS

B.1 Training Setting of Neural Solvers

Base Solver	Encoder layer	Batch Size	Sample Size	Epochs
AM	9	512	512×2500	600
POMO	6	64	100×1000	600

TABLE 5: Training configuration for AM [2] and POMO [5] on all COP.

For training neural solvers, the ASP framework runs the DE procedure (algorithm 1) or PSA procedure (algorithm 2) at each iteration, we run 5 iterations of the DE procedure and 1 iteration of PSA procedure, each iteration contains 5 training epochs. We train 100 iterations so the overall training epochs for the neural solver is 600. To make a fair comparison, in Table 2, 3 and 4, the results of POMO are obtained from the same training setting with POMO(ASP). For AM, we use the original training setting (encoder layer is equal to 3 and the number of training epochs is 100) and the pre-trained model parameters provided by the author because we find the performance of AM trained under the same setting (9 encoder layers and 600 epochs) with AM(ASP) is quite messy. We show the results in Appendix C. The specific setting of some key parameters is shown in Table 5.

B.2 Training Setting of Data Generator

We use Real-NVP [10] G_{γ} , a typical Normalizing Flow-based generative model to generate data distribution. Different COPs need the specification of the data generation process.

For TSP - In classical euclidean TSP, we only need to generate two-dimension coordinates. Specifically, we sample $x \sim \mathbf{U}([0, 1] \times [0, 1])$ and get data $y = G_{\gamma}(x) \sim P_{g, \gamma}$.

For VRP - Compared with TSP, the CVRP and SDVRP contain extra constraints on customer demand and vehicle capacity besides the two-dimension coordinates. In the general setting of applying neural solvers to solve CVRP and SDVRP, it’s common to set these constraints in a relatively safe manner. To avoid infeasible or bad instances due to the two constraints, we keep the generation of customer demand and vehicles the same as previous works [2] and focus on the impacts of euclidean coordinates. Same as TSP, we sample the customer and depot coordinates x from a two-dimension unit square and get data $y = G_\gamma(x) \sim P_{g,\gamma}$. **For PCTSP and SPCTSP** - We keep the same setting in AM [2] for the generation of prize and penalty and focus on the two-dimension coordinates as in TSP, VRP, and OP.

APPENDIX C FURTHER RESULTS OF AM

TABLE 6: Further results of AM with 9 encoder layers after training 600 epochs. The gap % is w.r.t. the best value across all methods.

		$n = 20$	$n = 40$	$n = 60$	$n = 80$	$n = 100$
TSP	AM-20	0.73%	2.09%	8.02%	12.33%	18.09%
	AM-50	83.35%	115.83%	150.54%	198.55%	235.07%
	AM-100	117.38%	165.39%	200.92%	281.61%	312.47%
CVRP	AM-20	3.64%	10.27%	19.01%	33.31%	31.38%
	AM-50	223.24%	277.00%	451.86%	407.61%	414.29%
	AM-100	223.24%	277.00%	451.86%	407.61%	414.29%
SDVRP	AM-20	3.35%	10.85%	17.20%	27.77%	28.38%
	AM-50	223.24%	277.00%	451.86%	407.61%	414.29%
	AM-100	148.69%	211.00%	254.66%	267.96%	297.00%
PCTSP	AM-20	0.26%	22.07%	53.28%	66.86%	81.58%
	AM-50	38.12%	15.11%	13.76%	7.14%	11.77%
	AM-100	148.69%	211.00%	254.66%	267.96%	297.00%
SPCTSP	AM-20	1.29%	21.77%	46.33%	63.09%	68.25%
	AM-50	38.12%	15.11%	13.76%	7.14%	11.77%
	AM-100	148.69%	211.00%	254.66%	267.96%	297.00%

In Table 6, we show the results of AM [2] trained from 9 encoder layers and 600 epochs on uniform distribution. AM-N means training AM under problem scale N and we evaluate AM-N on the generated instances with problem scales 20, 40, 60, 80, and 100. Results show that AM-50 and AM-100 work poorly due to the overfitting caused by the large training epochs. However, it’s interesting that AM-20 seems less affected by this problem.

APPENDIX D GENERALIZATION DEMONSTRATION

We show the generalization results of AM [2] and POMO [5] on different problem scales 20,30,40,50,60,70,80,90 and 100 in Fig. 9. On different problem scales, the base solver’s performance degrades as the difference becomes bigger, however, the base solver(ASP) can cover all the problem scales well.

APPENDIX E VISUALIZATION OF WEAKNESS DISTRIBUTION FOR TSP

In this part, we demonstrate the weakness distribution found by our data generator for TSP. From algorithm 1, the weakness distribution is

$$\mathbf{P}^n = \sum_i \sigma_{DG,i} \mathbf{P}_{\mathcal{I}^n,i}$$

where $\mathbf{P}_{\mathcal{I}^n,i}$ is the oracle of data generator trained at each PSRO iteration and $\sigma_{DG,i}$ is the meta-strategy. Thanks to the usage of Normalizing Flows, we can compute the probability exactly. The probability density function (pdf) is obtained within the range of $[0, 1] \times [0, 1]$. In Fig. 10, we can see that the weakness distributions for AM and POMO have an infinitesimal change over the uniform distribution, which can be seen as a specific type of data augmentation.

APPENDIX F FURTHER DEMONSTRATION OF LANDSCAPE

We use the “filter normalization” [60] to visualize the objective function curvature of COP in Fig. 11 and 12 for AM and POMO. We evaluate 1000 instances for each set of permuted parameters, the range of permutation is from -1 to 1 and the step is 50. We evaluate AM and POMO with the combination of the following settings:

- Different distributions: “Uni.” and “Mix Gau.” mean we plot the landscape of objective function evaluated on the instances sampling from uniform distribution and mix gaussian distribution
- Different training paradigm: “Neural solver(ASP)” means the results are obtained from the neural solver trained under the ASP framework, otherwise under the original setting
- Different problem scales: we evaluate neural solvers under different problem scales: 20, 50 and 100
- Different degrees of hardness: we separate the 1000 instances into three degrees of hardness according to the optimality gap: easy (instances of the first $\frac{1}{3}$ smallest optimality gap), median ($\frac{1}{3} \sim \frac{2}{3}$) and hard ($\frac{2}{3} \sim 1$).

For example, “AM(ASP)-20 on Mix Gau. (all)” means: the landscape is obtained by evaluating AM trained from ASP framework on TSP20 and the 1000 instances are sampled from mix gaussian distribution.

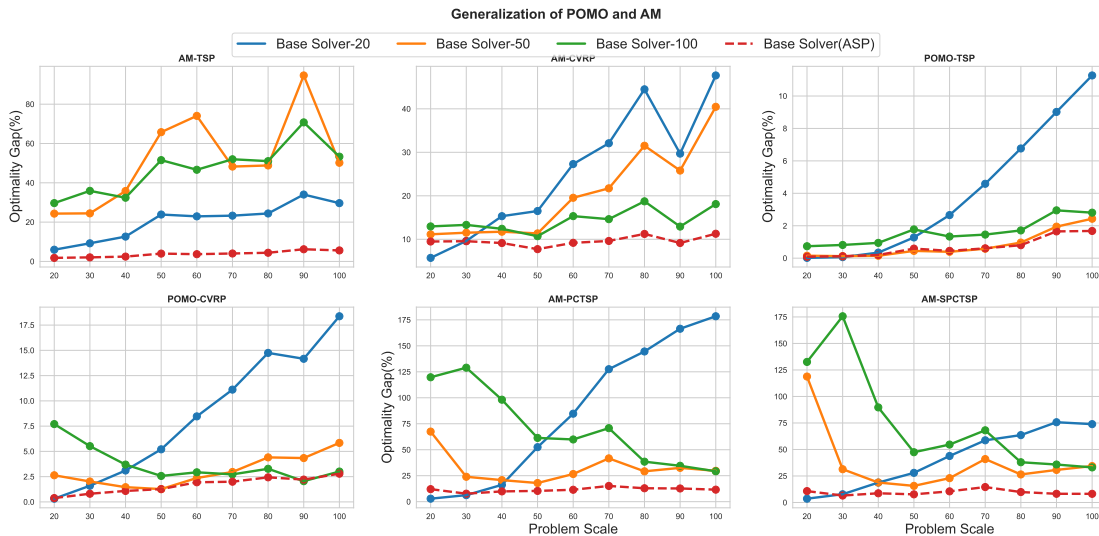


Fig. 9: Demonstration of generalization ability. Optimality gap(%) of AM and POMO as a function of problem scales $n \in \{20, 30, 40, 50, 60, 70, 80, 90, 100\}$. Results of Base Solver(ASP) are drawn using dashed lines while Base Solvers are drawn with a solid line. Intuitively, the dash (results of Base Solver(ASP)) line are approximately under all the solid lines (results of Base Solver).

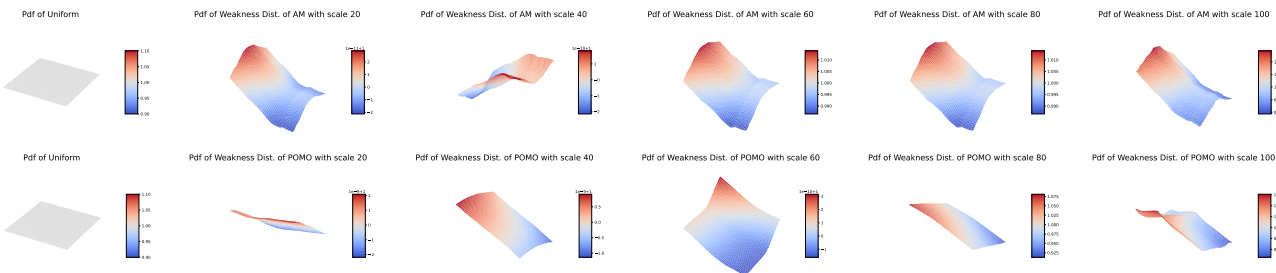


Fig. 10: Demonstration of weakness distribution for AM and POMO. The probability density function (pdf) is taken within the range of $[0, 1] \times [0, 1]$.



Fig. 11: All the landscapes of optimality gap (%) for AM.

Fig. 12: All the landscapes of optimality gap (%) for POMO.